

Sectional and projectional emittance measurementsa)

M. Sarstedt

Citation: [Review of Scientific Instruments](#) **67**, 1653 (1996); doi: 10.1063/1.1146910

View online: <http://dx.doi.org/10.1063/1.1146910>

View Table of Contents: <http://scitation.aip.org/content/aip/journal/rsi/67/4?ver=pdfcov>

Published by the [AIP Publishing](#)

Articles you may be interested in

[Development of an emittance meter and off-line measurements for the SPES project](#)

AIP Conf. Proc. **1423**, 482 (2012); 10.1063/1.3688849

[Portable emittance measurement devicea\)](#)

Rev. Sci. Instrum. **81**, 02B719 (2010); 10.1063/1.3267293

[Sediment tomography in the East China Sea: Compressional wave speed and attenuation inversions from mode travel time dispersion and Airy phase measurementsa\)](#)


J. Acoust. Soc. Am. **111**, 2388 (2002); 10.1121/1.4778117

[Sectional and projectional emittance measurements \(abstract\)a\)](#)


Rev. Sci. Instrum. **67**, 1271 (1996); 10.1063/1.1147241

[Single photon timing system for picosecond fluorescence lifetime measurementsa\)](#)

Rev. Sci. Instrum. **54**, 118 (1983); 10.1063/1.1137225



**Does your research require low temperatures? Contact Janis today.
Our engineers will assist you in choosing the best system for your application.**



10 mK to 800 K **LHe/LN₂ Cryostats**
Cryocoolers **Magnet Systems**
Dilution Refrigerator Systems
Micro-manipulated Probe Stations

sales@janis.com **www.janis.com**
Click to view our product web page.

Sectional and projectional emittance measurements^{a)}

M. Sarstedt

Lawrence Berkeley National Laboratory, University of California, 1 Cyclotron Road, Berkeley, California 94720

(Presented on 15 September 1995)

For many applications of ion sources the quality of the generated ion beam plays an increasingly important role. Ion sources consist of the plasma generator and the extraction system. Both parts can, due to high ion temperature or various aberrations, contribute to a degrading of the beam quality. Though the beam quality is determined by many more factors, the transverse motion of the particles certainly is one of the important parameters. Knowledge of it can be obtained by an emittance measurement. This is best done in a four-dimensional phase space, yielding a density distribution as function of the transverse spatial and momentum coordinates. Often, however, due to practical considerations, only two dimensions of the four-dimensional “trace space” are being measured. This two-dimensional data can be obtained as a section or as a projection of the four-dimensional trace space, where both methods have their merits. Projectional emittance measurements can usually be performed much easier and quicker, but by the projection of the four-dimensional space onto a two-dimensional plane information is lost. And although not all the particles of the beam are represented in a section of trace space, here aberrative distortions of the emittance can be seen most clearly and allow an easier comparison to numerically obtained data. The advantages and disadvantages of both methods are discussed. Numerical and experimental examples are presented. © 1996 American Institute of Physics. [S0034-6748(96)99202-9]

I. MOTIVATION

One major issue in the layout of any accelerator is the beam current and quality at the high-energy end of the system. A beam with as little disorder in the particle distribution as possible is therefore required. Since in any beamline, by itself this disorder can only increase, or at best stay unchanged, it is important to start the acceleration process with a beam of really good quality. This places high demands on the ion source and the initial acceleration steps, where, through finite ion temperature and possible lens aberrations, both the plasma generator and the extraction system can contribute to a degrading of the beam quality.

This beam quality is determined by the particle distribution in phase space, usually described by the emittance of the beam. There are various definitions of this quantity, all based on a characterization of the area in phase space covered by the density distribution of the phase space points.¹ One difficulty arises from the fact that the actual area of an assembly of points is always zero. Therefore, in all definitions of the emittance, either the intensity distribution has to be assumed as continuous, allowing an exact calculation of the fringe of the distribution, or the phase space has to be divided into small segments, then counting all segments that contain any number of points. The first is usually applied in a theoretical approach, whereas the second is used for numerical and experimental data.

As will be described in more detail, in computer simulations as well as in the representation of experimental data, two descriptions of the emittance of a beam are rather common. Both are derived from the particle distribution in four-

dimensional phase space, where one is a two-dimensional section of this phase space, the other one a projection onto a two-dimensional plane. Phase-space projections are in wide use for the calculation of beam dynamics in accelerator structures, e.g., in programs like PARMTEQ.² In programs for the calculation of ion optical lenses and extraction systems, e.g., IGUNE,³ often the distribution in phase-space sections is displayed. Thus, aberrations can be easily detected. Since for the design of accelerator structures both types of calculations are important and in use, an understanding has to be gained as to how the two representations are related and how a distribution in the rr' plane can be converted into the xx' plane.

II. THEORETICAL BACKGROUND

The development of an ensemble of particles in time can be described by the formalisms used in classical mechanics, and can be represented by the movement of one point in $6N$ -dimensional phase space, where N is the number of particles in the ensemble and the axes are given by the spatial and momentum coordinates x, y, z and p_x, p_y, p_z .⁴ For a more convenient description of the particles a projection into the six-dimensional phase space can be performed, yielding N points therein. The volume in phase space that is occupied by the density distribution $\rho_6(x, p_x, y, p_y, z, p_z)$ of the particles is a measure for the beam quality. For practical purposes often the six-dimensional phase space is separated into a two-dimensional longitudinal, and a four-dimensional transverse part. With the further assumption of a uniform particle momentum in longitudinal (z) direction, p_x and p_y can be replaced by the derivatives x' and y' , yielding the distribution function $\rho_4(x, x', y, y')$. This four-dimensional space is usually called trace space.

^{a)}The abstract for this paper appears in the Proceedings of the 6th International Conference on Ion Sources in Part II, Rev. Sci. Instrum. **67**, 1271 (1996).

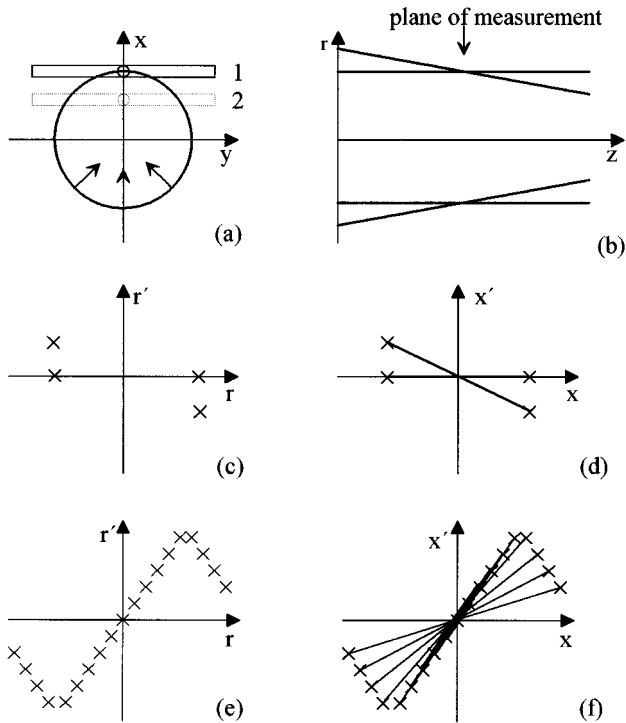


FIG. 1. Schematic representation of aberrations in a beam. (a) Hollow beam with two angular components (parallel and convergent) in xy plane. The convergent part is indicated by arrows. Two positions of measurement are pointed out. (b) In the rz plane the beams are crossing at the position of measurement. (c) rr' emittance, corresponding to measurement in (b). (d) xx' emittance. (e), (f) Transition of a homogeneous beam with aberrations from rr' to xx' plane.

To further reduce the dimensions of this trace space, it is possible to look at the xx' and the yy' distribution separately. For, e.g., the xx' plane, a two-dimensional section of the four-dimensional space yields $d_2(x, x') = \rho_4(x, x', 0, 0)$, while a projecting onto a two-dimensional plane is given by $\rho_2(x, x') = \iint \rho_4(x, x', y, y') dy dy'$.

The pattern of the points in trace space that represent the beam in the two different planes will henceforth be called rr' emittance or $\epsilon(rr')$ and xx' emittance or $\epsilon(xx')$, respectively. Note that since the rr' plane is a section of the four-dimensional space, the coordinate r can take on negative as well as positive values.

III. TRANSFORMATION FROM THE rr' PLANE TO THE xx' PLANE

A. Calculation of the weight function

For the transformation of the emittance from the rr' to the xx' plane a cylindrically symmetric beam is considered. For every two corresponding points in the rr' plane (representing an ideal hollow beam), a connecting line in the xx' plane is formed. In Fig. 1 such a hollow beam is shown schematically, containing two components of transverse momentum in the plane of measurement (b). Measurements in the rr' plane, performed with hole apertures (a), yield the distribution shown in (c), whereas a measurement with two slits (a), results in the distribution with connecting lines (d).

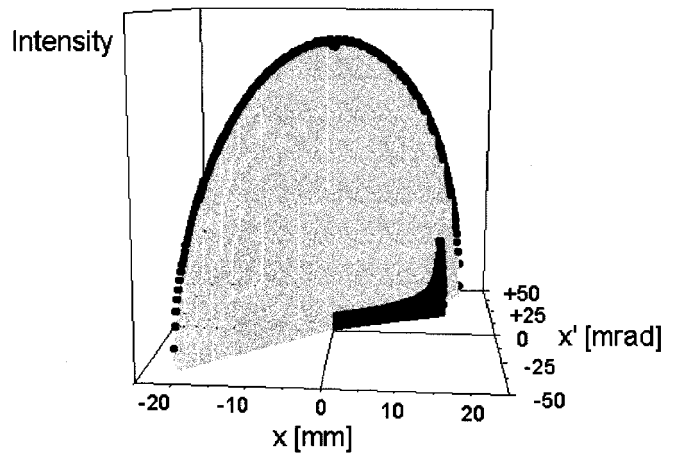


FIG. 2. Intensity as a function of x and x' for a beam similar to the example shown in Fig. 1(e), calculated for a finite slit width Δx_2 . Part of the intensity distribution of the connecting line of an aberrative beam (black) is in front of the main part of the distribution (light gray), crossing it at the origin. The continuation of this line is concealed behind it.

Without taking the finite slit width Δx into account, the weight function of these connecting lines can be calculated by describing the ideal hollow beam by a δ function in r . The result is given by Eq. (1). Here R describes the radius of the hollow beam, ρ_r is the line density of the current in the azimuthal direction, x is the position along the x axis, and $\rho(x)$ the resulting weight function along this connecting line:

$$\rho(x) = \frac{2\rho_r R}{(R^2 - x^2)^{1/2}}. \quad (1)$$

For a continuously filled beam, as schematically shown in Fig. 1(e), the connecting lines of trajectories with the same ratio of R' to R are overlaid and the intensities add up, indicated by the thicknesses of the lines (f). Beam aberrations, on the other hand, result in a filling of some of the formerly empty areas of trace space.^{5,6}

B. Influence of the first slit

For an xx' emittance measurement a slit has to be used that scans over the beam and defines the spatial position in trace space. The finite slit width leads to a modification of the weight function for the connecting lines [Eq. (2)]:

$$\rho(x, \Delta x) = \frac{1}{\Delta x} 2\rho_r R \left(\arcsin \frac{x + \Delta x/2}{R} - \arcsin \frac{x - \Delta x/2}{R} \right), \quad (2a)$$

$$\rho(x, \Delta x) = \frac{1}{\Delta x} 2\rho_r R \left(\arcsin 1 - \arcsin \frac{x - \Delta x/2}{R} \right). \quad (2b)$$

Part (a) of the equation is valid for the range $|x| \leq R - (\Delta x/2)$, part (b) for $R - \Delta x/2 \leq |x| \leq R + (\Delta x/2)$. Examples of these modified weight functions and consequences for the interpretation of measurements are discussed in Refs. 5 and 7.

For a beam similar to the example shown in Fig. 1(e), in Fig. 2 an intensity plot, i.e., the intensity as function of x and x' , is shown, calculated for a finite slit width Δx_2 . As de-

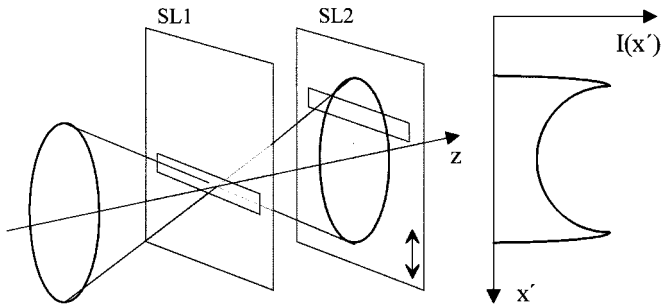


FIG. 3. For a hollow, convergent beam with its focal point at the position of the first slit, the same intensity distribution as discussed for the first slit applies here at the second slit.

scribed for the case of the initial weight function, here again the intensities of the overlaid connecting lines add up. For the aberrative part of the beam, however, the intensity distribution along the connecting line is directly given in Eq. (2). For better understanding, only one aberrative trajectory is considered. Part of the intensity distribution of the connecting line (black) is in front of the main part of the distribution (light gray), crossing it at the origin. The continuation of this line is concealed behind it.

A special case for these connecting lines arises, when such a hollow beam is convergent with its focal point at the position of the first slit. In this case, where the second slit essentially takes on the role of the first, the same intensity distribution as discussed above applies for the intensity distribution behind the second slit $\rho(x')$. Figure 3 demonstrates this schematically.

C. Influence of the second slit

Looking again at an ideal hollow beam, one can see that the part of it that is transmitted through the first slit has a certain extent in the x direction, simulating an unreal x' distribution at the second slit, and may also contain a real angular distribution for $R' \neq 0$. This leads to a widening of the connecting lines in the x' direction. At any position x an intensity distribution along x' can be found, so that a parallelogram is formed, as indicated in the xx' plane of Fig. 4. Similar to the case of the first slit, the finite width of the second slit again yields a modification of the density distribution in trace space. This is shown schematically in Fig. 5. At the position x_0 of the first slit the total intensity is given by $I(x_0) = \rho(x_0)\Delta x$. The second slit now scans across part of the distribution function $I(x)$, resulting in the new distribution function $I(x_0, x')$. Since the shape of this function is different for every position x , the overall intensity distribution $I(x, x')$ of the ideal hollow beam has a high degree of complexity. On the right side of Fig. 4 this intensity distribution is shown schematically for three positions along the x axis (R , 0 , and $-R$), with the intensity axis extending to the right. For $\Delta x_1 < R$, the width of the distribution in the x' direction, $\Delta x'$, is given by Eq. (3), where Δx_1 and Δx_2 denote the slit heights, Δz the distance between the two slits.

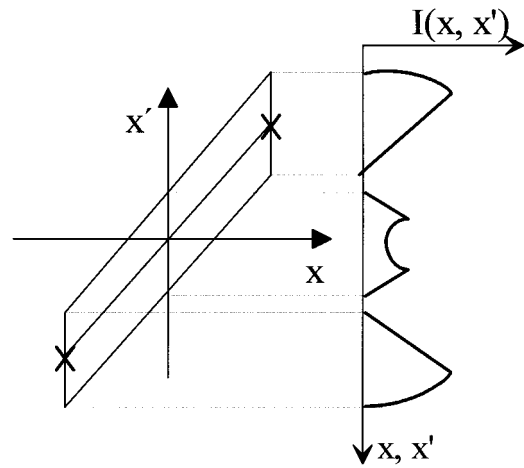


FIG. 4. The part of the beam that is transmitted through the first slit contains an x' distribution. At any position x an intensity distribution along x' can be found, forming a parallelogram. On the right side this intensity distribution is shown schematically for three positions along the x axis (R , 0 , and $-R$), with the intensity axis extending to the right.

$$\Delta x' = \Delta x_1 \frac{R'}{R} + \frac{\Delta x_1 + \Delta x_2}{\Delta z}. \quad (3)$$

For a parallel hollow beam ($R' = 0$), $\Delta x'$ becomes $(\Delta x_1 + \Delta x_2)/\Delta z$. For a divergent or convergent beam, $\Delta x'$ is a function of the R' of the initial hollow beam.

IV. DISCUSSION

There are essentially two ways to measure and represent two-dimensional emittance data, i.e., with sections or projections of the four-dimensional phase space. The method used should be chosen according to the requirements of the problem at hand. Knowledge about the effective emittance for example, often needed in accelerator physics, can be gained by both methods, since the changes to the emittance pattern in the transformation from the rr' to the xx' plane almost exclusively take place inside the fringes of the distribution. For knowledge about the exact shape of the aberrations as well as the exact density distribution, however, a closer look at the rr' emittance seems to be of advantage.

A comparison of an xx' and an rr' measurement of a highly distorted beam can be found in Ref. 5. This example demonstrates the severe loss of information due to the pro-

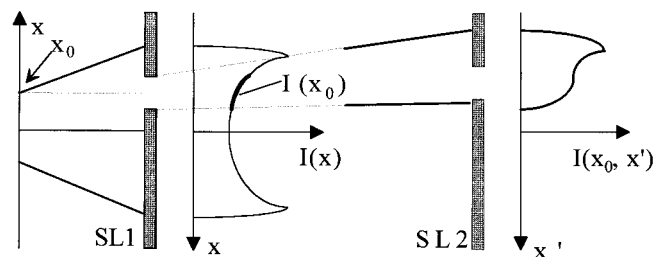


FIG. 5. Similar to the case of the first slit, the finite width of the second slit again yields a modification of the density distribution in trace space. At one position x_0 the second slit scans across part of the distribution function $I(x)$, resulting in the new distribution function $I(x_0, x')$.

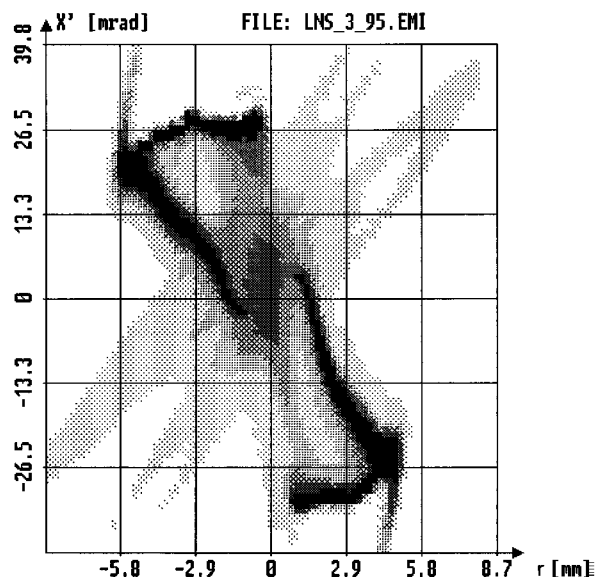


FIG. 6. Measurement of an “ rx ” emittance of a highly distorted beam. Although the method is much simpler than measurement of the rr' emittance, the aberrations can be clearly seen.

jection onto the xx' plane. It also shows the intensity distribution of the connecting lines as demonstrated in Fig. 2. Since measurements of the rr' plane usually are rather difficult to perform, one possibility to get a clearer look at the beam aberrations is a measurement in an “ rx ” plane,” meaning, only the first slit is replaced by a hole aperture, thus avoiding the integration over y but still integrating over y' . It should be pointed out, however, that no numerical emittance values can be obtained from this method. The result of such a measurement on the same beam as described in Ref. 5 can be seen in Fig. 6. It was taken with a modified slit–slit emittance measurement device,⁸ and displayed with the program PROEMI.⁹ Here, one part of the beam has a focal point at the position of the first aperture, the connecting line is almost parallel to the x' axis and can therefore be seen (integration over y'). The structure of the emittance pattern of the beam and even of the neutral particles in the beam (divergent part) is very obvious.

However, most often emittance measurements are performed in the xx' plane. In this case, in order to e.g. compare numerically calculated and experimentally obtained data, a transformation of the rr' emittance into an xx' emittance is indicated. In such a transformation two corresponding points in the rr' plane are connected by a line in the xx' plane.

It has been demonstrated here that the intensity distribution along the line depends on the width of the first slit, and that the width of the second slit results in a widening of this connecting line and a complex structure of the intensity distribution therein. The size of these areas around the connecting lines and their internal intensity distribution obviously have an influence on the values calculated for the area emittance as well as for the rms emittance. For a comparison to experimental data the transformation therefore should be done under consideration of the geometrical properties of the measuring device used.

ACKNOWLEDGMENTS

For helpful discussions I would like to thank R. Becker, H. Klein, and R. Thomae from the University of Frankfurt, Germany, and C. F. Chan, W. Kunkel, and J. Staples from the Lawrence Berkeley National Laboratory, California. This work was supported by the BMFT and the HMWK through the University of Frankfurt, Germany, and by the Director, Office of Basic Energy Sciences, Advanced Energy Projects Division of the U.S. Department of Energy under Contract No. DE-AC03-76SF00098.

¹C. Lejeune and J. Aubert, *Emittance and Brightness: Definitions and Measurements*, Institut d'Electronique Fondamentale, Université Paris, France (1980).

²H. Deaven and K. Chan, *Computer Codes for Particle Accelerator Design and Analysis: A Compendium*, LA-UR-90-1766, 142 (1990).

³R. Becker and W. Herrmannsfeldt, *Rev. Sci. Instrum.* **63**, 2756 (1992).

⁴A. J. Lichtenberg, *Phase-Space Dynamics of Particles* (Wiley, New York, 1969).

⁵M. Sarstedt *et al.*, *Nucl. Instrum. Methods B* **99**, 721 (1995).

⁶C. F. Chan *et al.*, *Nucl. Instrum. Methods A* **306**, 112 (1991).

⁷M. Sarstedt, Dissertation, University of Frankfurt, Frankfurt, Germany (1994).

⁸G. Riehl and M. Sarstedt, GSI-91-27, 49 (1991).

⁹G. Riehl, Dissertation, University of Frankfurt, GSI-93-43 (1993).